Genetic Dissection of Horizontal Cell Inhibitory Signaling in Mice in Complete Darkness In Vivo

Bruce A. Berkowitz,[1,2] Geoffrey G. Murphy,[3] Cheryl Mae Craft,[4] D. James Surmeier,[5] and Robin Roberts[1]

[1]Department of Anatomy and Cell Biology, Wayne State University School of Medicine, Detroit, Michigan, United States
[2]Department of Ophthalmology, Wayne State University School of Medicine, Detroit, Michigan, United States
[3]University of Michigan Medical School, Molecular Behavioral Neuroscience Institute, Molecular and Integrative Physiology, Ann Arbor, Michigan, United States
[4]Mary D. Allen Laboratory for Vision Research, USC Eye Institute, and Department of Ophthalmology and Department of Cell and Neurobiology, Keck School of Medicine of the University of Southern California, Los Angeles, California, United States
[5]Department of Physiology, Feinberg School of Medicine, Northwestern University, Chicago, Illinois, United States

Purpose. To test the hypothesis that horizontal cell (HC) inhibitory signaling controls the degree to which rod cell membranes are depolarized as measured by the extent to which L-type calcium channels (LTCCs) are open in complete darkness in the mouse retina in vivo.

Methods. Dark-adapted wild-type (wt), *CACNA1F* ($Ca_v1.4^{-/-}$), arrestin-1 ($Arr1^{-/-}$), and *CACNA1D* ($Ca_v1.3^{-/-}$) C57Bl/6 mice were studied. Manganese-enhanced MRI (MEMRI) evaluated the extent that rod LTCCs are open as an index of loss of HC inhibitory signaling. Subgroups were pretreated with D-*cis*-diltiazem (DIL) at a dose that specifically antagonizes $Ca_v1.2$ channels in vivo.

Results. Knockout mice predicted to have impaired HC inhibitory signaling ($Ca_v1.4^{-/-}$ or $Arr1^{-/-}$) exhibited greater than normal rod manganese uptake; inner retinal uptake was also supernormal. Genetically knocking out a closely associated gene not expected to impact HC inhibitory signaling (*CACNA1D*) did not generate this phenotype. The $Arr1^{-/-}$ mice exhibited the largest rod uptake of manganese. Manganese-enhanced MRI of DIL-treated $Arr1^{-/-}$ mice suggested a greater number of operant LTCC subtypes (i.e., $Ca_v1.2$, 1.3, and 1.4) in rods and inner retina than that in DIL-treated $Ca_v1.4^{-/-}$ mice (i.e., $Ca_v1.3$). The $Ca_v1.3^{-/-}$ + DIL-treated mice exhibited evidence for a compensatory contribution from $Ca_v1.2$ LTCCs.

Conclusions. The data suggest that loss of HC inhibitory signaling is the proximate cause leading to maximally open LTCCs in rods, and possibly inner retinal cells, in mice in total darkness in vivo, regardless of compensatory changes in LTCC subtype manifested in the mutant mice.

Keywords: manganese-enhanced MRI, inhibitory signaling, L-type calcium chananels

L-type calcium channels (LTCCs) are the major calcium entry path into rod cells, which make up approximately 97% of photoreceptors in mice.[1–3] In the dark, rod cell membranes are depolarized, resulting in the sustained opening of synaptic LTCCs of the $Ca_v1.4$ subtype and presumably $Ca_v1.3$ LTCCs in rod nuclei.[4–6] Persistent opening of $Ca_v1.4$ channels triggers continuous release of the neurotransmitter glutamate.[7] Exocytosis at the photoreceptor synapse is also modulated by the synaptic interaction between arrestin-1 and N-ethylmaleimide sensitive factor.[8] Just anterior to the photoreceptor synapse, retinal interneuron horizontal cells (HCs), which express LTCCs, receive glutamatergic input from photoreceptors, resulting in depolarization of their plasma membrane.[9] Horizontal cell depolarization produces, by as yet an unclear mechanism, inhibitory signaling whose target on photoreceptors are $Ca_v1.4$ channels.[10] Our current understanding of proteins that regulate glutamatergic-evoked HC inhibitory signaling to photoreceptors (i.e., $Ca_v1.4$ and arrestin-1) is mainly based on light-based studies ex vivo. It is unclear if these proteins are also at play in mice in total darkness in vivo when HCs experience a maximum and sustained glutamate exposure.

The degree to which rod LTCCs are open or closed in vivo can be objectively evaluated by measuring specific uptake of Mn^{2+}, which is an LTCC probe, using manganese-enhanced MRI (MEMRI), the imaging modality of choice for noninvasively studying retinal ion homeostasis.[11] Because Mn^{2+} efflux from cells is slow compared with influx,[12] the extent of accumulation a few hours after injection is a useful measure of manganese influx. Manganese-enhanced MRI relies on the well-defined laminar structure of the retina to distinguish, for example, inner retinal uptake from outer retinal uptake.[13–18] In the outer retina, the dominant photoreceptor cells in the mouse retina are the rods.[1] Thus, uptake of manganese from 50% to 88% depth into the retina primarily reflects a single cell type. We recently directly demonstrated that MRI has the resolution to, for example, distinguish between inner segments and outer segments, based on the light-evoked expansion of the subretinal space in mice and rats.[19,20] On the other hand, MEMRI cannot differentiate among MEMRI signals in the inner retina, where there is substantial overlap of several different cell types, including HCs. In any event, uptake is increased by rod cell membrane depolarization (i.e., opening of LTCCs with

dark adaptation versus being closed in the light) and the LTCC-specific agonist Bay K 8644 in light-adapted animals.[21-23] Rod cell uptake is strongly inhibited in the dark by LTCC-specific blockers, such as nifedipine,[24] and D-*cis*-diltiazem (DIL).[25] Importantly, MEMRI uniquely measures layer-specific retinal LTCC activity in complete darkness that was encoded while mice were awake and freely moving.

Here, using MEMRI and genetically modified mice, we test the hypothesis that HC inhibitory signaling controls the degree to which rod cell membranes are depolarized as measured by the extent to which LTCCs are open in complete darkness in the mouse retina in vivo. In the dark, polarization of the rod cell membrane (and thus the degree to which associated LTCCs are open) reflects a balance of two competing signals: a depolarization signal generated from the outer segments (which will open LTCCs) and a hyperpolarization signal generated from HCs (which will close LTCCs). If, for example, HC inhibitory signaling were completely absent, the depolarization signal would dominate and LTCCs will be maximally open. In this study, we examined $Ca_v1.4$ and arrestin-1, two proteins that normally regulate the release of glutamate, an essential condition that engages HC inhibitory signaling in bright and dim light. Our prediction was that in each knockout mouse, HC inhibitory signaling would be impaired and LTCCs would be open to a greater extent than normal. We also predicted that the absence of $Ca_v1.3$, a channel not known to regulate glutamate release, would not produce a supernormal uptake phenotype.

METHODS

All animals were treated in accordance with the National Institutes of Health Guide for the Care and Use of Laboratory Animals, the ARVO Statement for the Use of Animals in Ophthalmic and Vision Research, and Institutional Animal and Care Use Committee authorization. Animals were housed and maintained in 12 hour:12 hour light–dark cycle laboratory lighting, unless otherwise noted.

Groups and Treatment

The following age-matched groups, a mix of male and female mice, were studied: (1) untreated C57Bl/6J mice (wild-type [wt], Jackson Laboratories, Bar Harbor, ME, USA; these data have been previously published[26]); (2) $Ca_v1.4^{-/-}$ mice, breeding pairs were originally provided by Marion Maw, University of Otago[27] (Dunedin, New Zealand) and then kindly provided by Amy Lee, University of Iowa (Iowa City, IA, USA); (3) all knockout mice null for $Ca_v1.3$, breeding pairs were originally provided by Jörg Striessnig, University of Innsbruck (Innsbruck, Austria), including knockout mice on C57Bl/6J or C57BL/6/SVEV129 F2 hybrid backgrounds[28]; (4) arrestin-1 knockouts, $Arr1^{-/-}$ (kind gift from Jeanne Chen, University of Southern California, Los Angeles, CA, USA)[29]; these animals were maintained in the dark at all times to prevent degeneration.[30] Mice also were treated with either vehicle (saline) or DIL (30 mg/kg, subcutaneously injected, Sigma D2521; Sigma-Aldrich Corp., St. Louis, MO, USA) 30 minutes before manganese injection.[26] The rationale for using DIL as a specific antagonist against the $Ca_v1.2$ LTCC subtype is presented in the discussion.

Manganese-Enhanced MRI

The MEMRI procedure in mice has been described in detail previously.[13] Briefly, all animals were maintained in darkness for 16 to 20 hours before manganese injection. For the dark-adapted study, all procedures (e.g., weighing, injecting vehicle/drugs/$MnCl_2$, anesthetic administration, and MRI examination)

were performed under dim red light or darkness. For the light-adapted study, mice were brought into the light approximately 20 minutes before manganese injection. In treated mice, vehicle or drug was injected 30 minutes before $MnCl_2$ injection. The $MnCl_2$ was administered as an intraperitoneal (IP) injection (66 mg $MnCl_2 \cdot 4H_2O$/kg) on the right side of awake mice. There is no evidence that doses of $MnCl_2$ in the range from 44 to 66 mg/kg IP alter histology, visual performance, blood-barrier integrity, visual behavior, or electrophysiology.[14,17,18,31-33] After this injection, animals were maintained in dark or light conditions for another 3.5 to 4.0 hours. Immediately before the MRI experiment, animals were anesthetized with urethane (36% solution IP; 0.083 mL/20 g animal weight, prepared fresh daily; Sigma-Aldrich, Milwaukee, WI, USA) and 2% lidocaine drops applied. The MRI data were acquired on a 7T system (Clinscan; Bruker, Billerica, MA, USA). Retinal partial saturation T_1 data were acquired using a dual-coil mode on a 7T Bruker Clinscan system. Several single spin-echo (time to echo 13 ms, 7×7 mm², matrix size 160×320, slice thickness 600 μm, in-plane resolution 21.875 μm) images were acquired at different repetition times (TRs) in the following order (number per time between repetitions in parentheses): TR 0.15 s (6), 3.50 s (1), 1.00 s (2), 1.90 s (1), 0.35 s (4), 2.70 s (1), 0.25 s (5), and 0.50 s (3). To compensate for reduced signal/noise ratios at shorter TRs, progressively more images were collected as the TR decreased.

Please note that MRI data do not allow ready visualization of cells within retinal layers, as is possible from optical coherence tomography. Instead, layer locations are inferred based on the retina's well-defined laminar structure, clear anatomical landmarks, like the vitreous–retina border, and highly localized functional changes within the retina. Thus, at the present resolution, we previously demonstrated that MRI can distinguish inner segments from outer segments based on the light-evoked expansion of the subretinal space surrounding the outer segments in mice and rats, as well as, for example, inner from outer retina manganese uptake as a function of light, DIL-induced suppression of only inner retinal manganese uptake, and the outer nuclear layer–only tetrameric visual arrestin-1 and its reduction via light-evoked translocation.[19,20,26,34] Collectively, these examples strongly support our claim that the resolution of MRI is sufficient for extracting meaningful layer-specific functional data in vivo.

Manganese-enhanced MRI data from the central retinal (± 1 mm from the center of the optic nerve) were analyzed as previously described.[13] Single images acquired with the same TR were first registered (rigid body) and then averaged. These averaged images were then registered across TRs. The same regions of interest as above were analyzed by calculating $1/T_1$ maps by first fitting to a three-parameter T_1 equation ($y = a + b*(\exp[-c*TR])$, where a, b, and c are fitted parameters on a pixel-by-pixel basis using R (v.2.9.0; R Foundation for Statistical Computing, Vienna, Austria) scripts developed in-house, and the minpack.lm package (v.1.1.1; Timur V. Elzhov and Katharine M. Mullen minpack.lm: R interface to the Levenberg-Marquardt nonlinear least-squares algorithm found in MINPACK, R package version 1.1–1). The reciprocal ($1/T_1$) values directly reflect manganese levels. Central intraretinal $1/T_1$ profiles were obtained as detailed elsewhere.[14] Values from the superior and inferior retina were averaged. Only those animals that took up manganese above baseline (i.e., 0.6 s⁻¹) were included in the final analysis.[31]

In each mouse, retinal thicknesses (μm) from the MEMRI images were objectively determined using the "half-height method," wherein a border is determined via a computer algorithm based on the crossing point at the midpoint between the local minimum and maximum, as detailed elsewhere.[14,35] The distance between two neighboring crossing-points thus
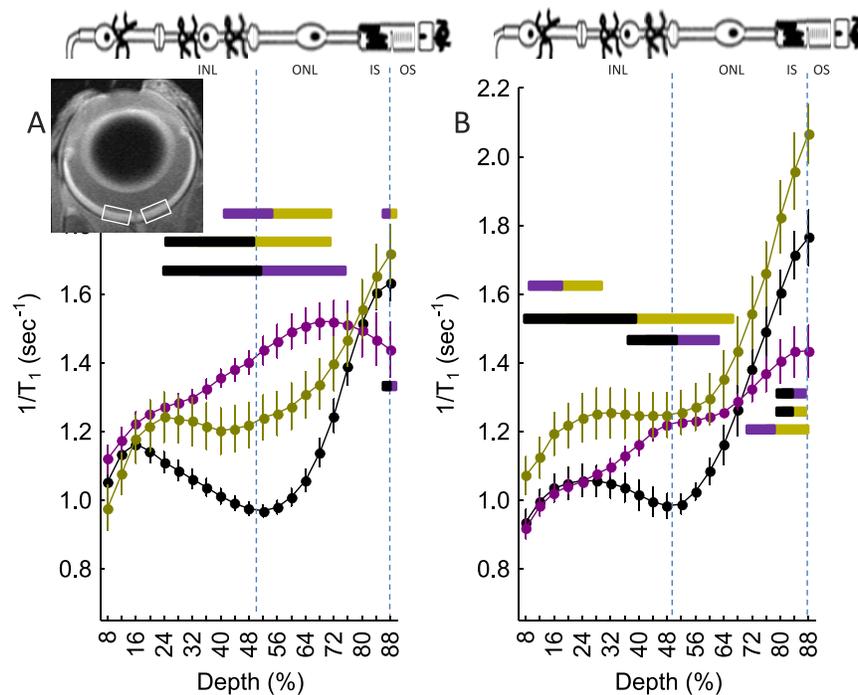
FIGURE 1. Degree of retinal LTCC opening as measured by extent of manganese uptake in vivo and impact of DIL: central (± 0.4–1.0 mm from the optic nerve head, illustrated by the *white boxes* in the *inset image*) retinal manganese uptake (as evaluated via $1/T_1$) profiles of (**A**) dark-adapted wt mice (*closed black circles*, $n = 19$), $Ca_v1.4^{-/-}$ mice (*closed gold circles*, $n = 5$), $Arr1^{-/-}$ mice (*closed magenta circles*, $n = 5$), and (**B**) DIL-treated wt, $Ca_v1.4^{-/-}$, and $Arr1^{-/-}$ mice (color scheme as in [**A**]). Data are shown as a function of distance from the retina/nonretina borders, where 0% is the vitreous/retina border and 100% is the retina/choroid border. Regions near borders are not shown because these regions likely include some signal from outside of the retina (i.e., partial volume averaging with vitreous or choroid/sclera). *Bicolored lines* above profiles indicate retinal regions with significant ($P < 0.05$) differences in manganese uptake between control and experimental mice indicated by the color. *Above graph*: Simplified schematic of retina and support circulations.[66-68] The retina has a well-defined laminar structure that allows us to reasonably label, on high-resolution MEMRI (21.9-μm axial resolution),[23] regions of uptake at 24% to 50% depth as the inner nuclear layer, at 50% to 68% depth as rod nuclei, at 68% to 88% depth as the rod inner segment region, and >88% as the rod outer segment region.

represents an objectively-defined thickness. Thickness values were then normalized with 0% depth at the presumptive vitreoretinal border and 100% depth at the presumptive retina–choroid border. Once normalized, the outer plexiform layer was considered to be located at 50% and inner/outer segment division at 88%, based on optical coherence tomography data.[14,19,34] Within the profile of each mouse, because of partial volume averaging, each pixel contains contributions from its nearest neighbor, and we are confident in these assignments to within approximately 10%, on the normalized thickness scale. For example, there are slight contributions from nonretinal tissue anteriorly at the vitreoretinal border and posteriorly at the retina–choroid border. The latter contribution was previously demonstrated with gadolinium-based measurements.[17] We typically exclude the anterior (0%–8% depth) and posterior (88%–100% depth) regions on the basis of this partial volume-averaging argument.[14,36]

Note that MEMRI provides a profile across the retina (i.e., transretinally) that allows measurement of uptake in rod cells as well as in cells of the inner retina. We rule out limited spatial resolution of the images, and the associated partial volume averaging between inner and outer nuclear layers (see above), as a concern based on the following argument. Assume for the sake of the argument that only the outer nuclear layer takes up more manganese than in wt mice and that the inner retina uptake is not different from wt values. In this case, one expects an asymmetrical uptake at approximately the 50% depth regardless of partial volume averaging. However, the supernormal uptake was observed symmetrically at approximately the 50% depth (Fig. 1). This symmetry argues that greater than normal

manganese uptake occurs in both outer and inner retina. Nonetheless, because the literature on HC inhibitory signaling to cells of the inner retina is far less developed than that for photoreceptors, the physiologic interpretation of a supernormal uptake into cells of the inner retina is somewhat unclear.

Optokinetic Tracking (OKT)

Two visual performance metrics were evaluated in awake and freely moving mice: spatial frequency thresholds (SFT; "acuity," in cycles/degree [c/d]) and contrast sensitivity (CS; measured at the peak of the nominal curve [0.06 c/d], inverse Michelson contrast [unitless]) using the optokinetic tracking reflex (OptoMotry; CerebralMechanics, Inc., Lethbride, AB, Canada).[37] In brief, a vertical sine wave grating is projected as a virtual cylinder in three-dimensional coordinate space on computer monitors arranged in a quadrangle around a testing arena. After an overnight dark adaptation, unrestrained mice are placed on an elevated platform at the center of the arena. An experimenter used a video image of the arena from above to view the animal and follow the position of its head with the aid of a computer mouse and a crosshair superimposed on the frame. The X–Y positional coordinates of the crosshair centered the hub of the virtual cylinder, enabling its wall to be maintained at a constant "distance" from the animal's eyes, and thereby to fix the spatial frequency (SF) of the stimulus at the animal's viewing position. When the cylinder was rotated in the clockwise (CW) or counter-clockwise (CCW) direction and the animal followed with head and neck movements that tracked the rotation, it was judged that the animal's visual
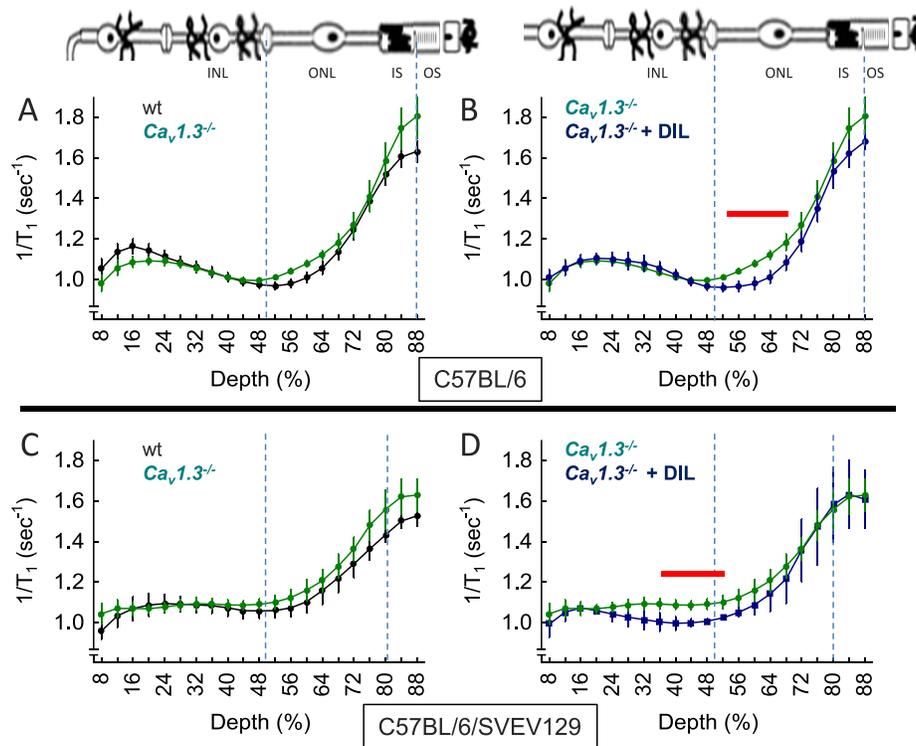
FIGURE 2. Extent of LTCC opening as measured by MEMRI in $Ca_v1.3^{-/-}$ mice and impact of DIL in vivo. Retinal manganese uptake profiles of dark-adapted wt mice (*closed black circles*), $Ca_v1.3^{-/-}$ mice (*closed green circles*), or $Ca_v1.3^{-/-}$ mice + DIL treatment (*closed blue circles*) on either a C57Bl/6J background (*top row*) or C57BL/6/SVEV129 F2 hybrid background (*bottom row*). (**A**) Wild-type ($n = 19$) versus $Ca_v1.3^{-/-}$ ($n = 5$) mice, (**B**) $Ca_v1.3^{-/-}$ ($n = 5$) versus $Ca_v1.3^{-/-}$ mice + DIL treatment ($n = 5$), (**C**) wt ($n = 5$) versus $Ca_v1.3^{-/-}$ ($n = 5$) mice, and (**D**) $Ca_v1.3^{-/-}$ ($n = 5$) versus $Ca_v1.3^{-/-}$ mice + DIL treatment ($n = 3$). Graphs are presented using the conventions in Figure 1. *Red lines* above profiles indicate retinal regions with significant ($P < 0.05$) differences in manganese uptake between control and experimental mice indicated.

system could distinguish the grating. Clockwise and CCW tracking provides a measure of left and right eye SFT and CS.[37] One set of SFT and CS measurements can reliably be obtained in 30 minutes. Optokinetic tracking visual performance assessment was performed 1 day before MEMRI examination.

Statistical Analysis

The OKT data were consistent with a normal distribution and were compared using a one-way ANOVA analysis with post hoc two-tailed *t*-test analyses. Comparisons of MEMRI uptake data between groups were performed using individual *t*-tests at different locations of the intraretinal profiles. A generalized estimating equation approach also was used to compare selected location ranges identified from the *t*-tests as significant.[18,38] A generalized estimating equations performs a general linear regression analysis using contiguous locations in each subject and accounts for the within-subject correlation between contiguous locations. In all cases, $P \leq 0.05$ was considered statistically significant. Data are presented as mean ± SEM unless otherwise noted.

RESULTS

$Ca_v1.4$ LTCCs

We first examined the $Ca_v1.4$ LTCC subtype because it is solely localized to photoreceptor synaptic terminals, is critical for modulating the release of glutamate at the photoreceptor synapse, and is the likely LTCC target of HC inhibitory signaling.[2,4,39,40] For these reasons, we hypothesized that in

the absence of $Ca_v1.4$ channels, HC inhibitory signaling does not occur. Cone-based phototopic visual performance (OKT) was completely absent in $Ca_v1.4^{-/-}$ mice (data not shown). Consistent with this hypothesis, we found that dark-adapted mice null for $Ca_v1.4$ channels had a greater than normal (i.e., supernormal) uptake of manganese in the outer nuclear layer (and cells of the inner retina [presented below]) (Fig. 1A). In the outer nuclear layer, in the absence of $Ca_v1.4$ channels in rods, manganese enters via a combination of $Ca_v1.2$ and $Ca_v1.3$ channels.[3,26,41]

$Ca_v1.3$ LTCCs

Because of a lack of an established $Ca_v1.3$-specific antagonist and specific antibodies,[42] we indirectly tested for a $Ca_v1.2$ and $Ca_v1.3$ contributions using $Ca_v1.2$-specific DIL treatment. Manganese uptake was not ($P > 0.05$) suppressed in the DIL-treated dark-adapted $Ca_v1.4$ null mice in the inner plexiform, inner nuclear, and outer nuclear layers (Fig. 1B), suggesting that $Ca_v1.3$ channels (previously suggested to be DIL-insensitive) represent a likely dominant influx route for manganese in these mice.[3,31,41] Supernormal uptake also was noted in a small region of the outer segment region; however, because LTCCs have not been reported in this region, the interpretation of this change is currently unclear again. Nonetheless, these results are consistent with previous suggestions that loss of $Ca_v1.4$ channels results in compensatory upregulation of rod $Ca_v1.3$ LTCCs.[3,41]

Because $Ca_v1.3$ LTCCs appeared to be the dominant functional LTCC in the $Ca_v1.4^{-/-}$ mice, we asked what role $Ca_v1.3$ might normally play in HC inhibitory signaling. Dark-adapted $Ca_v1.3^{-/-}$ mice on a C57Bl/6 background normally express $Ca_v1.4$ channels,[43] and had a normal transretinal

TABLE. Summary of Cone-Based Visual Performance Testing

Group	n	Strain	SFT, c/d	CS, Unitless
wt	21	C57Bl/6	0.418 ± 0.003	19.0 ± 0.5
$Ca_v1.3^{-/-}$	17	C57Bl/6	0.392 ± 0.008*	19.9 ± 1.0
$Ca_v1.3^{-/-}$	2	C57Bl/6/SVEV129 F2 hybrid	0.416 ± 0.004	21.6 ± 3.4
$Arr1^{-/-}$	4	C57Bl/6	0.124 ± 0.036*	4.5 ± 2.7*

* $P < 0.05$ compared with wt.

uptake profile (Fig. 2). We also investigated $Ca_v1.3^{-/-}$ mice on a C57BL/6/SVEV129 F2 hybrid background. Although the overall uptake profile was different from that on the C57BL/6 background, it was also not altered by elimination of $Ca_v1.3$ channels (Figs. 2A, 2C). Because a supernormal uptake phenotype was not observed in $Ca_v1.3^{-/-}$ mice of either strain, it appears that $Ca_v1.3$ channels do not contribute to, or are the target of, HC inhibitory signaling.

Cone-based phototopic CS was normal in $Ca_v1.3^{-/-}$ mice on the C57Bl/6 background (Table). The SFT was lower in the knockout compared with wt mice, but CS was normal. However, the small apparent decrease in SFT was likely due to the very tight error bars and is likely not physiologically relevant. Knockout mice on the C57BL/6/SVEV129 F2 hybrid background also appeared to have normal visual performance, although the number of animals studied was too low to provide meaning statistical comparisons.

Next we checked if, in the absence of $Ca_v1.3$ channels, $Ca_v1.2$ channels were upregulated, as previously noted in other neuronal tissue.[44] $Ca_v1.3$ null mice were treated with DIL and found to have a focal suppression of uptake, suggesting localized upregulation of $Ca_v1.2$ channels in both strains (Figs. 2B, 2D); interestingly, the retinal regions affected by DIL were strain dependent (Figs. 2B, 2D). Although the reason underlying these strain differences is not clear, these data nonetheless suggest that $Ca_v1.3$ channels are functionally important enough that the $Ca_v1.2$ subtype is compensatory expressed.

Inner Retina

We noted that the inner retina of the $Ca_v1.4$ null mice also had a greater than normal uptake (Fig. 1); this greater than normal uptake was unresponsive to DIL treatment (Fig. 1). These data suggest that $Ca_v1.3$ channels are the predominate type of LTCCs in these mice, even in regions of the inner retina that are normally associated with $Ca_v1.2$.[26] Functionally, these mutant mice have a reported greatly diminished b-wave[39]; however, ERG largely reports on movement of monovalent ions and not changes in influx via calcium channels.[31] The MEMRI data raise the possibility that HC inhibitory "feed-forward" signaling is also disrupted in the $Ca_v1.4$ knockout mice, although more work is needed to unravel the contribution of the different cell types in the inner retina.[45,46]

Arrestin-1

In dark-adapted mice, arrestin-1 is located in the outer nuclear layer/inner segment regions where it plays an essential role in modulating glutamate exocytosis at the photoreceptor synapse; however, with light exposure, arrestin-1 translocates to the outer segments, binds to phosphorylated opsins, and terminates G-protein–coupled photo-transduction signaling.[47] In $Arr1^{-/-}$ mice, $Ca_v1.4$ channels are fully expressed and functional to the best of our knowledge, although because exocytosis, and thus release of glutamate, is impaired,[8] we speculated that HC inhibitory signaling was not engaged; cone-based photopic visual performance was absent in $Arr1^{-/-}$ mice

(Table). Consistent with this hypothesis, on MEMRI examination, dark-adapted $Arr1^{-/-}$ mice demonstrated a greater than normal uptake in rod nuclei (Fig. 1A); a small region in the outer segment region also showed differences whose interpretation at this time is unclear. We also found a greater than normal uptake in the inner retina of the arrestin-1 null mice (Fig. 1A). This result suggests a role for HC inhibitory "feed-forward" signaling although additional work remains to understand this phenomenon.[45,46]

Notably, as seen in Figure 1, the extent of uptake in the $Arr1^{-/-}$ mice was even greater than in the $Ca_v1.4^{-/-}$ mice (Fig. 1A). We tested the idea that this may be due to a different array of LTCC subtypes between these two mice. The $Arr1^{-/-}$ mice treated with DIL exhibited a significant suppression of manganese uptake, particularly in the inner plexiform layer (similar in extent to that in wt mice), but remained supernormal in the inner and outer nuclear layers after treatment (Fig. 1B); a difference also was noted in the outer segment region for a currently unclear reason. These data support our present spatial resolution as adequate for monitoring localized changes within the retina. In addition, these results suggest that there are contributions from a DIL-sensitive component (likely $Ca_v1.2$ channels) and a DIL-insensitive component (likely $Ca_v1.3$ and $Ca_v1.4$ channels). Thus, the greater uptake in the $Arr1^{-/-}$ mice appears to be due to a greater number of influx pathways than in the $Ca_v1.4$ mice, in which only $Ca_v1.3$ LTCCs seem to operate.

DISCUSSION

The purpose of HC inhibitory signaling in bright light is most commonly understood in terms of controlling cone-generated synaptic gain and lateral inhibition onto cone cells forming the basis of the center-surround organization of vision.[45,46] In dim light, HC inhibitory signaling onto rod cells also has been documented and suggested to fulfill these same two purposes.[2,4,39,40] However, until the present study, the presence of HC inhibitory signaling onto rods in full darkness had not been investigated. Horizontal cell inhibitory signaling to the inner nuclear layer in the light also has been suggested previously, but remains relatively poorly studied compared with HC inhibitory signaling onto photoreceptors.[45,46] Intriguingly, cells of the inner nuclear layer mirrored the uptake pattern in the rod cells in all models, suggesting a role for HC inhibitory signaling into the inner retina in complete darkness.

In total darkness, we speculate that HC inhibitory signaling acts to throttle down the extent of LTCC opening to regulate how much calcium enters into rod (and possibly cells of the inner retina). It was beyond the scope of this study to investigate the exact mechanism(s) by which HCs communicate with photoreceptors, a currently active area of research by other laboratories, or inner retina.[45,46] Nonetheless, in this study, data from different genetically engineered knockout mouse models suggest for the first time the occurrence of HC inhibitory signaling in total darkness involving proteins previously identified as regulating HC inhibitory signaling to photoreceptors in the light (Fig. 3).

The $Ca_v1.4$ channels are located only at the photoreceptor synapse and play an essential role in vision because $Ca_v1.4^{-/-}$ mice are blind and mutations in the *CACNA1F* gene, which encode $Ca_v1.4$ LTCC α1 subunits, are linked with loss of vision in Åland Island eye disease, cone-rod dystrophy, X-linked retinal disorder, night blindness–associated transient tonic down-gaze, and incomplete congenital stationary night blindness.[2,3,5,39,43,48-50] In contrast, the functional role of $Ca_v1.3$ channels is less clear, in part because current antibodies for identifying these channels and used for immunological

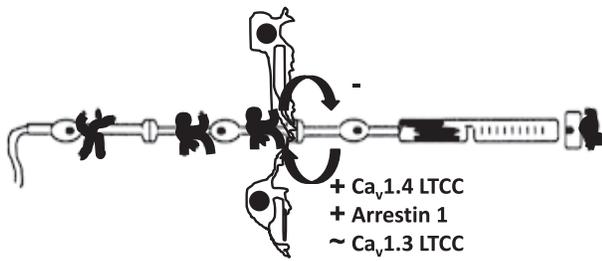+ Ca$_v$1.4 LTCC
+ Arrestin 1
~ Ca$_v$1.3 LTCC

FIGURE 3. Simplified schematic representation highlighting the targets studied. Illustration of the retina and support circulations (using conventions in Fig. 1), including the HCs.[66-68] In the dark, rod cell membranes are depolarized, resulting in the sustained opening of synaptic LTCCs of the Ca$_v$1.4 subtype and presumably Ca$_v$1.3 LTCCs in rod nuclei.[4-6] Persistent opening of Ca$_v$1.4 channels (but not, apparently, Ca$_v$1.3 LTCCs) triggers continuous release of the neurotransmitter glutamate, a process regulated by arrestin-1.[7,8] When HCs receive glutamatergic input, their membranes depolarize and send (by a yet unclear process) inhibitory signals back to the photoreceptors.[9,10] The present data suggest that the target proteins chosen (based on light-based studies ex vivo) also participate in inhibitory signaling in mice in total darkness in vivo when HCs experience a maximum and sustained glutamate exposure.

localization are nonspecific and a selective antagonist has not yet been established.[42] The Ca$_v$1.3 channels have been documented in cells of the inner retina and in RPE cells based on electrophysiological evidence, and their mRNA exists in rod cells and cells of the inner retina.[3,41,42,51-53] However, *Ca$_v$1.3$^{-/-}$* mice do not exhibit an impaired visual phenotype as measured by electrophysiology and water maze testing.[54,55] The present data suggest that that apparent lack of phenotype may be due to compensatory upregulation of retinal Ca$_v$1.2 channels, an idea not previously tested in *Ca$_v$1.3$^{-/-}$* mice.[44] The remaining major LTCC found in neurons, Ca$_v$1.2, is located at the inner plexiform and ganglion layers but not rod cells in young mice, although in older mice, Ca$_v$1.2 LTCCs appear to be functional in the outer retina in vivo.[26,43]

In this study, we also found evidence that rod cells in vivo exhibit the potential for a remarkably flexible repertoire of LTCC subtypes. These data appear to be in line with previous observations of LTCC plasticity in aging and disease states.[24,26,31] It is not currently clear why one LTCC subtype becomes operant and another does not, as each subtype occupies a distinct biophysical niche.[7] For example, in this study, rod cells of *Ca$_v$1.4$^{-/-}$* mice seemed to express functional Ca$_v$1.3 but not Ca$_v$1.2 channels, even though rod Ca$_v$1.2 channels appear to become functional in the absence of arrestin-1. Nor is it understood why different retinal regions appear to demonstrate a strain-dependent LTCC plasticity (Fig. 2). Nonetheless, the present results, and data from other studies, raise the possibility that the array of rod LTCC subtypes can vary, and this insight may help resolve discordant reports of the efficacy of the Ca$_v$1.2-specific antagonist DIL in, for example, different retinal degeneration models.[24,26,31,56] Furthermore, because rod cell calcium overload via increased calcium influx is commonly thought to promote retinal degeneration, mapping the repertoire of retinal LTCC subtypes in vivo using MEMRI will likely help guide calcium channel therapy.[57]

Different laboratories have generated half maximal inhibitory concentration (IC50) DILs by using expressed channels in cells, suggesting that there is some subtype specificity (i.e., IC50 approximately 45 μM [Ca$_v$1.2] versus approximately 326 μM [Ca$_v$1.3] and approximately 92 μM [Ca$_v$1.4]).[5,26,31,58,59] However, the exact DIL IC50s for the LTCC subtypes in the retina in vivo are not known.[26,31] Nonetheless, we find spatial agreement using DIL with MEMRI, between where Ca$_v$1.2 is

located on immunohistochemistry (inner retina) and DIL-induced focal suppression of manganese uptake in the inner retina.[5,26,31,58,59] Ca$_v$1.3 is thought to be more widely expressed than just inner retina and we find no evidence for DIL-related suppression in other parts of the retina of wt mice.[3] In addition, when Ca$_v$1.3 expression increases in the retina with age, a substantially greater amount of DIL is needed to suppress manganese uptake relative to that in younger rat retinas.[31] Together, these data in vivo are consistent with the notion that Ca$_v$1.3 channels respond to DIL differently from Ca$_v$1.2 channels.[60,61] We also suggest that if DIL antagonized Ca$_v$1.4 channels, it would be expected, based on the *Ca$_v$1.4$^{-/-}$* mice data herein (Fig. 1), that the uptake of manganese would be supernormal. A supernormal uptake in rod cells was not seen in the C+DIL mice. Collectively, these considerations support the use of DIL as an antagonist for Ca$_v$1.2 in unraveling LTCCs in vivo using MEMRI.[31]

Here, deletion of Ca$_v$1.3 did not result in a supernormal uptake phenotype in the F2 hybrid mice, which demonstrates that this observation is not unique to the C57BL/6 genetic background. Although we did observe some strain-dependent differences in the localized upregulation of Ca$_v$1.2, it is widely appreciated that genetic background significantly influences mouse behavior and physiology.[62] In particular, there have been a number of reports suggesting an interaction between altered ion channel function and genetic background that lead to striking endophenotypes.[63-65] The present data are consistent with this literature.

The in vivo aspect of the hypothesis tested herein could not have been evaluated using otherwise powerful electrophysiological approaches that document rod cell voltage–current relationships in single cells or in postmortem tissue. Furthermore, it is difficult to translate electrophysiological data into actual function in the awake animal. Thus, MEMRI provides a useful and complementary approach that extends our ability to evaluate rod LTCC function into the fully dark-adapted, awake, and freely moving mouse in vivo. The available evidence suggests that Ca$_v$1.2 and Ca$_v$1.3 subtypes are both capable of transporting manganese in vivo, although the unique biophysical properties of each channel suggests that under the same conditions the extent of manganese influx will vary with the subtype.[31,61] The high sequence homology between Ca$_v$1.3 and Ca$_v$1.4 channels suggests that manganese can enter via Ca$_v$1.4 LTCCs.[60] In addition, we note that manganese accumulates intracellularly in all layers of the retina 3.5 to 4.0 hours after injection, and thus is expected to have had access to the LTCCs.[18] Combining MEMRI with genetically modified mice and a specific LTCC subtype antagonist provided a degree of mechanistic specificity.

In summary, the combination of MEMRI, genetically modified mice, and DIL treatment was shown to be a powerful and useful approach for investigating LTCCs and HC inhibitory signaling in awake and freely moving dark-adapted mice in vivo. Because reductions in HC inhibitory signaling in the mutant mice is expected to cause the balance of rod cell membrane depolarization/hyperpolarization signals to chronically deviate from that in mice with intact HC inhibitory signaling, we reasoned that the complement of LTCC subtypes used by the rod cell might also deviate from that in normal mice.[24,26,31] In fact, the present evidence suggests that all of the examined knockout mice had their rod LTCCs manifest altered to different degrees. In turn, the number and type of LTCC subtype expressed will modify the amount of manganese entering into the rod cell. Nonetheless, loss of HC inhibitory signal appears to be the proximate cause leading to maximally open LTCCs in rods, regardless of subtype.

Acknowledgments

Disclosure: **B.A. Berkowitz**, None; **G.G. Murphy**, None; **C.M. Craft**, None; **D.J. Surmeier**, Genetech (C), Merck (C), Pfizer (C), Teva (C); **R. Roberts**, None

References

1. Carter-Dawson LD, Lavail MM, Sidman RL. Differential effect of the rd mutation on rods and cones in the mouse retina. *Invest Ophthalmol Vis Sci*. 1978;17:489–498.

2. Morgans CW, Gaughwin P, Maleszka R. Expression of the alpha1F calcium channel subunit by photoreceptors in the rat retina. *Mol Vis*. 2001;7:202–209.

3. Xiao H, Chen X, Steele EC Jr. Abundant L-type calcium channel Ca(v)1.3 (alpha1D) subunit mRNA is detected in rod photoreceptors of the mouse retina via in situ hybridization. *Mol Vis*. 2007;13:764–771.

4. Schmitz Y, Witkovsky P. Dependence of photoreceptor glutamate release on a dihydropyridine-sensitive calcium channel. *Neuroscience*. 1997;78:1209–1216.

5. Baumann L, Gerstner A, Zong X, Biel M, Wahl-Schott C. Functional characterization of the L-type Ca2+ channel cav1.4alpha1 from mouse retina. *Invest Ophthalmol Vis Sci*. 2004;45:708–713.

6. Johansen O, Vaaler S, Jorde R, Reikeras O. Increased plasma glucose levels after Hypnorm anaesthesia, but not after Pentobarbital anaesthesia in rats. *Lab Anim*. 1994;28:244–248.

7. McRory JE, Hamid J, Doering CJ, et al. The CACNA1F gene encodes an L-type calcium channel with unique biophysical properties and tissue distribution. *J Neurosci*. 2004;24:1707–1718.

8. Huang SP, Brown BM, Craft CM. Visual arrestin 1 acts as a modulator for N-ethylmaleimide-sensitive factor in the photoreceptor synapse. *J Neurosci*. 2010;30:9381–9391.

9. Schubert T, Weiler R, Feigenspan A. Intracellular calcium is regulated by different pathways in horizontal cells of the mouse retina. *J Neurophysiol*. 2006;96:1278–1292.

10. Liu X, Hirano AA, Sun X, Brecha NC, Barnes S. Calcium channels in rat horizontal cells regulate feedback inhibition of photoreceptors through an unconventional GABA- and pH-sensitive mechanism. *J Physiol*. 2013;591:3309–3324.

11. Ramos de Carvalho JE, Verbraak FD, Aalders MC, van Noorden CJ, Schlingemann RO. Recent advances in ophthalmic molecular imaging. *Surv Ophthalmol*. 2014;59:393–413.

12. Tofts PS, Porchia A, Jin Y, Roberts R, Berkowitz BA. Toward clinical application of manganese-enhanced MRI of retinal function. *Brain Res Bull*. 2010;81:333–338.

13. Berkowitz BA, Bissig D, Patel P, Bhatia A, Roberts R. Acute systemic 11-*cis*-retinal intervention improves abnormal outer retinal ion channel closure in diabetic mice. *Mol Vis*. 2012;18:372–376.

14. Bissig D, Berkowitz BA. Same-session functional assessment of rat retina and brain with manganese-enhanced MRI. *Neuroimage*. 2011;58:749–760.

15. Berkowitz BA, Roberts R, Bissig D. Light-dependant intraretinal ion regulation by melanopsin in young awake and free moving mice evaluated with manganese-enhanced MRI. *Mol Vis*. 2010;16:1776–1780.

16. Berkowitz BA, Roberts R, Oleske DA, et al. Quantitative mapping of ion channel regulation by visual cycle activity in rodent photoreceptors in vivo. *Invest Ophthalmol Vis Sci*. 2009;500:1880–1885.

17. Berkowitz BA, Roberts R, Luan H, et al. Manganese-enhanced MRI studies of alterations of intraretinal ion demand in models of ocular injury. *Invest Ophthalmol Vis Sci*. 2007;48:3796–3804.

18. Berkowitz BA, Roberts R, Goebel DJ, Luan H. Noninvasive and simultaneous imaging of layer-specific retinal functional adaptation by manganese-enhanced MRI. *Invest Ophthalmol Vis Sci*. 2006;47:2668–2674.

19. Bissig D, Berkowitz BA. Light-dependent changes in outer retinal water diffusion in rats in vivo. *Mol Vis*. 2012;18:2561–2xxx.

20. Berkowitz BA, Grady EM, Khetarpal N, Patel A, Roberts R. Oxidative stress and light-evoked responses of the posterior segment in a mouse model of diabetic retinopathy. *Invest Ophthalmol Vis Sci*. 2015;56:606–615.

21. Drapeau P, Nachshen DA. Manganese fluxes and manganese-dependent neurotransmitter release in presynaptic nerve endings isolated from rat brain. *J Physiol*. 1984;348:493–510.

22. Carlson RO, Masco D, Brooker G, Spiegel S. Endogenous ganglioside GM1 modulates L-type calcium channel activity in N18 neuroblastoma cells. *J Neurosci*. 1994;14:2272–2281.

23. Berkowitz BA, Bissig D, Dutczak O, Corbett S, North R, Roberts R. MRI biomarkers for evaluation of treatment efficacy in preclinical diabetic retinopathy. *Expert Opin Med Diagn*. 2013;7:393–403.

24. Berkowitz BA, Bissig D, Bergman D, Bercea E, Kasturi VK, Roberts R. Intraretinal calcium channels and retinal morbidity in experimental retinopathy of prematurity. *Mol Vis*. 2011;17:2516–2526.

25. Berkowitz BA, Roberts R, Penn JS, Gradianu M. High-resolution manganese-enhanced MRI of experimental retinopathy of prematurity. *Invest Ophthalmol Vis Sci*. 2007;48:4733–4740.

26. Berkowitz BA, Grady EM, Roberts R. Confirming a prediction of the calcium hypothesis of photoreceptor aging in mice. *Neurobiol Aging*. 2014;35:1883–1891.

27. Hemara-Wahanui A, Berjukow S, Hope CI, et al. A CACNA1F mutation identified in an X-linked retinal disorder shifts the voltage dependence of Cav1.4 channel activation. *Proc Natl Acad Sci U S A*. 2005;102:7553–7558.

28. Platzer J, Engel J, Schrott-Fischer A, et al. Congenital deafness and sinoatrial node dysfunction in mice lacking class D L-type Ca2+ channels. *Cell*. 2000;102:89–97.

29. Chen J, Simon MI, Matthes MT, Yasumura D, LaVail MM. Increased susceptibility to light damage in an arrestin knockout mouse model of Oguchi disease (stationary night blindness). *Invest Ophthalmol Vis Sci*. 1999;40:2978–2982.

30. Brown BM, Ramirez T, Rife L, Craft CM. Visual arrestin 1 contributes to cone photoreceptor survival and light adaptation. *Invest Ophthalmol Vis Sci*. 2010;51:2372–2380.

31. Bissig D, Goebel D, Berkowitz BA. Diminished vision in healthy aging is associated with increased retinal L-type voltage gated calcium channel ion influx. *PLoS One*. 2013;8:e56340.

32. Holt, Ag, Bissig D, Mirza, N, Rajah, G, Berkowitz B. Evidence of key tinnitus-related brain regions documented by a unique combination of manganese-enhanced MRI and acoustic startle reflex testing. *PLoS One*. 2010;5:e14260.

33. Berkowitz BA, Roberts R, Stemmler A, Luan H, Gradianu M. Impaired apparent ion demand in experimental diabetic retinopathy: correction by lipoic acid. *Invest Ophthalmol Vis Sci*. 2007;48:4753–4758.

34. Berkowitz BA, Gorgis J, Patel A, et al. Development of an MRI biomarker sensitive to tetrameric visual arrestin 1 and its

reduction via light-evoked translocation in vivo. *FASEB J.* 2015;29:554–564.

35. Cheng H, Nair G, Walker TA, et al. Structural and functional MRI reveals multiple retinal layers. *Proc Natl Acad Sci U S A.* 2006;103:17525–17530.

36. Berkowitz BA, Bissig D, Ye Y, Valsadia P, Kern TS, Roberts R. Evidence for diffuse central retinal edema in vivo in diabetic male Sprague Dawley rats. *PLoS One.* 2012;7:e29619.

37. Douglas RM, Alam NM, Silver BD, McGill TJ, Tschetter WW, Prusky GT. Independent visual threshold measurements in the two eyes of freely moving rats and mice using a virtual-reality optokinetic system. *Vis Neurosci.* 2005;22:677–684.

38. Liang Z. Longitudinal data analysis using generalized linear models. *Biometrika.* 1986;73:13–22.

39. Mansergh F, Orton NC, Vessey JP, et al. Mutation of the calcium channel gene Cacna1f disrupts calcium signaling, synaptic transmission and cellular organization in mouse retina. *Hum Mol Genet.* 2005;14:3035–3046.

40. Babai N, Thoreson WB. Horizontal cell feedback regulates calcium currents and intracellular calcium levels in rod photoreceptors of salamander and mouse retina. *J Physiol.* 2009;587:2353–2364.

41. Morgans CW, Bayley PR, Oesch NW, Ren G, Akileswaran L, Taylor WR. Photoreceptor calcium channels: insight from night blindness. *Vis Neurosci.* 2005;22:561–568.

42. Zou J, Lee A, Yang J. The expression of whirlin and Cav1.3alpha1 is mutually independent in photoreceptors. *Vision Res.* 2012;75:53–59.

43. Busquet P, Khoi Nguyen N, Schmid E, et al. CaV1.3 L-type Ca2+ channels modulate depression-like behaviour in mice independent of deaf phenotype. *Int J Neuropsychopharmacol.* 2010;13:499–513.

44. Jurkovicova-Tarabova B, Griesemer D, Pirone A, Sinnegger-Brauns MJ, Striessnig J, Friauf E. Repertoire of high voltage-activated Ca2+ channels in the lateral superior olive: functional analysis in wild-type, Ca(v)1.3(-/-), and Ca(v)1.2DHP(-/-) mice. *J Neurophysiol.* 2012;108:365–379.

45. Yang XL, Wu SM. Feedforward lateral inhibition in retinal bipolar cells: input-output relation of the horizontal cell-depolarizing bipolar cell synapse. *Proc Natl Acad Sci U S A.* 1991;88:3310–3313.

46. Thoreson WB, Mangel SC. Lateral interactions in the outer retina. *Prog Retin Eye Res.* 2012;31:407–441.

47. Zhang H, Huang W, Zhang H, et al. Light-dependent redistribution of visual arrestins and transducin subunits in mice with defective phototransduction. *Mol Vis.* 2003;9:231–237.

48. Burtscher V, Schicker K, Novikova E, et al. Spectrum of Cav1.4 dysfunction in congenital stationary night blindness type 2. *Biochim Biophys Acta.* 2014;1838:2053–2065.

49. Koschak A, Reimer D, Walter D, et al. cav1.4alpha1 subunits can form slowly inactivating dihydropyridine-sensitive L-type Ca2+ channels lacking Ca2+-dependent inactivation. *J Neurosci.* 2003;23:6041–6049.

50. Strom TM, Nyakatura G, Apfelstedt-Sylla E, et al. An L-type calcium-channel gene mutated in incomplete X-linked congenital stationary night blindness. *Nat Genet.* 1998;19:260–263.

51. Habermann CJ, O'Brien BJ, Wässle H, Protti DA. AII amacrine cells express L-type calcium channels at their output synapses. *J Neurosci.* 2003;23:6904–6913.

52. Rosenthal R, Thieme H, Strauss O. Fibroblast growth factor receptor 2 (FGFR2) in brain neurons and retinal pigment epithelial cells act via stimulation of neuroendocrine L-type channels (Ca(v)1.3). *FASEB J.* 2001;15:970–977.

53. Xu HP, Zhao JW, Yang XL. Expression of voltage-dependent calcium channel subunits in the rat retina. *Neurosci Lett.* 2002;329:297–300.

54. Wu J, Marmorstein AD, Striessnig J, Peachey NS. Voltage-dependent calcium channel CaV1.3 subunits regulate the light peak of the electroretinogram. *J Neurophysiol.* 2007;97:3731–3735.

55. McKinney BC, Murphy GG. The L-Type voltage-gated calcium channel Cav1.3 mediates consolidation, but not extinction, of contextually conditioned fear in mice. *Learn Mem.* 2006;13:584–589.

56. Barabas P, Cutler PC, Krizaj D. Do calcium channel blockers rescue dying photoreceptors in the Pde6b (rd1) mouse? *Adv Exp Med Biol.* 2010;664:491–499.

57. Fox DA, Poblenz AT, He L, Harris JB, Medrano CJ. Pharmacological strategies to block rod photoreceptor apoptosis caused by calcium overload: a mechanistic target-site approach to neuroprotection. *Eur J Ophthalmol.* 2003;13:S44–S56.

58. Tarabova B, Lacinova L, Engel J. Effects of phenylalkylamines and benzothiazepines on Cav1.3-mediated Ca2+ currents in neonatal mouse inner hair cells. *Eur J Pharmacol.* 2007;573:39–48.

59. Glossmann H, Linn T, Rombusch M, Ferry DR. Temperature-dependent regulation of d-cis-[3H]diltiazem binding to Ca2+ channels by 1,4-dihydropyridine channel agonists and antagonists. *FEBS Lett.* 1983;160:226–232.

60. Lipscombe D, Helton TD, Xu W. L-type calcium channels: the low down. *J Neurophysiol.* 2004;92:2633–2641.

61. Xu W, Lipscombe D. Neuronal CaV1.3alpha1 L-type channels activate at relatively hyperpolarized membrane potentials and are incompletely inhibited by dihydropyridines. *J Neurosci.* 2001;21:5944–5951.

62. Crawley JN, Belknap JK, Collins A, et al. Behavioral phenotypes of inbred mouse strains: implications and recommendations for molecular studies. *Psychopharmacology (Berl).* 1997;132:107–124.

63. Miller AR, Hawkins NA, McCollom CE, Kearney JA. Mapping genetic modifiers of survival in a mouse model of Dravet syndrome. *Genes Brain Behav.* 2014;13:163–172.

64. Connor JX, McCormack K, Pletsch A, et al. Genetic modifiers of the Kv beta2-null phenotype in mice. *Genes Brain Behav.* 2005;4:77–88.

65. Buchner DA, Trudeau M, Meisler MH. SCNM1, a putative RNA splicing factor that modifies disease severity in mice. *Science.* 2003;301:967–969.

66. Wangsa-Wirawan ND, Linsenmeier RA. Retinal oxygen: fundamental and clinical aspects. *Arch Ophthalmol.* 2003;121:547–557.

67. Zhi Z, Chao JR, Wietecha T, Hudkins KL, Alpers CE, Wang RK. Noninvasive imaging of retinal morphology and microvasculature in obese mice using optical coherence tomography and optical microangiography. *Invest Ophthalmol Vis Sci.* 2014;55:1024–1030.

68. Paques M, Tadayoni R, Sercombe R, et al. Structural and hemodynamic analysis of the mouse retinal microcirculation. *Invest Ophthalmol Vis Sci.* 2003;44:4960–4967.